



## International Journal of Mechanical and Sustainability Engineering Technology

Journal homepage:

<https://uniexpertsacademy.com/index.php/IJMSET/index>

ISSN: 3083-8363



# Operation Mechanisms and Scalable Manufacturing Methods for Perovskite Solar Cells: A Review

Hawraa Fadhel<sup>1</sup>, Zainab mohammed<sup>1</sup>, Dhafer Manea Hachim<sup>1</sup>, Rahul Johari<sup>2,\*</sup>

<sup>1</sup> Dept. of Mechanical Engineering Techniques of Power, Engineering Technical College of Najaf, Al- Furat Al-Awsat Technical University, Najaf 31001, Iraq

<sup>2</sup> Department of Applied Sciences and Humanities, Jamia Millia Islamia, New Delhi 110025, India.

### ARTICLE INFO

#### Article history:

Received 2 August 2025

Received in revised form 7 December 2025

Accepted 31 December 2025

Available online 04 April 2026

#### Keywords:

Perovskite Solar Cells, Power Conversion Efficiency, Low-Cost Fabrication, Tunable Bandgap, Electron Transport Layer

### ABSTRACT

This review explores the working principles and manufacturing techniques of perovskite solar cells (PSCs), a fast-growing and highly promising area in solar energy research. In recent years, PSCs have attracted considerable attention because of their high efficiency, affordable fabrication, and versatile material properties. What makes them stand out is their ability to convert sunlight into electricity efficiently using lightweight, low-cost, and flexible materials that are easier and cheaper to process than traditional silicon-based cells. With the increasing global demand for clean and renewable energy, PSCs offer a promising pathway to affordable and scalable solar power. Studies have shown that the use of methylammonium lead iodide ( $\text{CH}_3\text{NH}_3\text{PbI}_3$ ), a commonly used perovskite material, together with an appropriate device design, can result in energy conversion efficiencies of up to 3.81%, supported by high incident photon-to-current efficiency (IPCE) and short-circuit current density (Jsc). Further improvements have been achieved using zinc oxide (ZnO) films with a thickness of 440 nm, which demonstrated an efficiency of 10.8% due to their porous structure and excellent electron transport properties. Additionally, three-dimensional nanocomposites combining mesoporous titanium dioxide ( $\text{TiO}_2$ ) with  $\text{CH}_3\text{NH}_3\text{PbI}_3$  have been found to significantly enhance performance. Doping  $\text{TiO}_2$  with nickel further improved the system by raising the Fermi level and enhancing charge mobility in the electron transport layer, thereby enabling more efficient charge transport within the device. Moreover, PSCs are compatible with a range of fabrication methods, including spin coating, inkjet printing, and roll-to-roll processing, which are cost-effective and suitable for large-scale production. This manufacturing flexibility opens the door to applications such as flexible solar panels, solar fabrics, building-integrated solar modules, and portable energy solutions. In summary, the ongoing development of new materials and structures, together with innovations in scalable manufacturing, continues to improve the performance, stability, and commercial potential of perovskite solar cells, making them one of the most exciting technologies for the future of clean energy.

\* Corresponding author.

E-mail address: [rahuljohari.phy@gmail.com](mailto:rahuljohari.phy@gmail.com)

## 1. Introduction

Halide perovskites are promising solar materials because of their high efficiency and low cost. Originating from the broader perovskite family, they have rapidly advanced from an efficiency of 3.8% in 2009 to over 25% today, rivaling silicon cells. Their rapid progress and versatility have attracted global interest, highlighting their potential in clean energy [1]. Ahmed H. Ali et al. [2] reported that perovskite solar cells have undergone rapid development since their emergence, surpassing 25% efficiency in just over a decade. This progression highlights their potential to compete with conventional silicon-based photovoltaics. Unlike traditional reviews, this paper emphasizes a critical analysis of device performance and highlights current research gaps. With global electricity demand expected to exceed 30 TW by 2050, perovskite technology is uniquely positioned to deliver scalable and cost-effective clean energy.

According to Priyanka Roy et al. [3], the rising global electricity demand, expected to increase from 16 TW to over 30 TW by 2050, makes it crucial to develop clean, affordable, and scalable energy sources. Relying solely on fossil fuels will not be sufficient, and solar energy is one of the most promising alternatives. Halide perovskite solar cells (PSCs) stand out because they can absorb sunlight very efficiently using very thin layers of material. This is due to their high absorption coefficients. As noted by Di Zhou et al. [5], perovskites require less material to absorb sunlight and can efficiently transport charge because of their long carrier lifetimes and diffusion lengths. Their adjustable bandgap also enables broader light absorption, supporting high-efficiency multi-junction solar cells.

The manufacturing process of perovskite solar cells is also far more accessible than that of conventional silicon cells. As explained by Akihiro Kojima et al. [8], perovskite cells can be fabricated using low-cost methods such as spin coating and dual-source evaporation in simple laboratory settings, enabling flexible and portable applications. Yaoguang Rong et al. [10] conducted accelerated aging tests to better understand how and why these materials degrade over time, thereby offering insights into how their stability can be improved. Martin A. Green et al. [11] also discussed the technical and economic barriers that must be resolved before perovskites can be widely adopted in the market.

To address these issues, many researchers have turned to advanced material and device engineering. For instance, Juan-Pablo Correa-Baena et al. [12] explored ion-engineering techniques to enhance charge selectivity and minimize energy losses. Abdulaziz S. R. Bati et al. [13] proposed integrating perovskite cells with other photovoltaic systems to boost overall efficiency. Meanwhile, Jin Young Kim et al. [14] investigated how the theoretical Shockley-Queisser limit might be surpassed by designing multi-layer or tandem cells that combine perovskites with other semiconductors. Interface and device structure optimization has also been a major focus, with Naveen Kumar Elumalai et al. [15] offering a comprehensive overview of how interfaces can be improved for better charge transfer and stability. Furthermore, Ajay Kumar Jena et al. [16] emphasized the development of lead-free and all-inorganic perovskite alternatives, which are safer for the environment and exhibit improved thermal and chemical stability. Other researchers, such as Victoria Gonzalez-Pedro [17], have demonstrated the vital role of  $\text{CH}_3\text{NH}_3\text{PbX}_3$  in efficient charge collection and suggested optimization techniques based on diffusion length measurements.

The NREL Best Research-Cell Efficiencies chart illustrates the evolution of solar cell technologies, highlighting record-setting efficiency milestones across different photovoltaic (PV) technologies from 1975 to 2025. Halide perovskite-based tandem solar cells, particularly perovskite/silicon cells, have recently surged ahead, achieving efficiencies above 30% and narrowing the gap with the long-dominant III-V multijunction cells. The chart illustrates a competitive landscape in which institutions such as FhG-ISE, HZB, Oxford PV, and NREL lead innovation across diverse technologies, including

perovskites, organic cells, quantum dots, and multijunction III-V devices. Top-performing solar cell architectures, such as six-junction III-V multijunction cells, have reached record efficiencies nearing 48%, albeit often under concentrated illumination, underscoring their potential for space and specialized terrestrial applications. While traditional crystalline silicon continues to improve incrementally, emerging technologies, especially perovskite tandems, show rapid efficiency gains, reflecting their potential to revolutionize commercial photovoltaic systems as shown in Figure 1 [20].

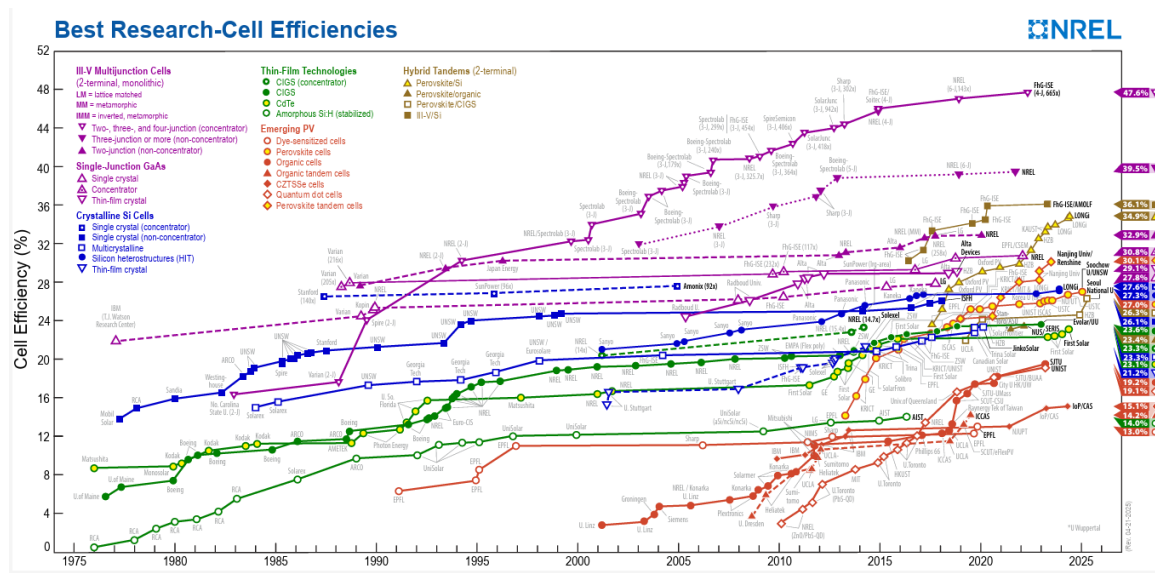


Figure 1. Efficiency diagram by NREL [15]

This study presents an overview of the manufacturing processes and operational mechanisms of perovskite solar cells. In recent years, these cells have attracted considerable interest because of advances in fabrication techniques and the development of diverse material systems.

Although perovskite solar cells have achieved efficiencies exceeding 25% within a decade, their rapid progress must be considered alongside intrinsic instability issues, such as ion migration and moisture sensitivity, which continue to limit their operational lifetime. Recent modelling studies have shown that their high absorption coefficients and long carrier diffusion lengths are highly favourable for thin-film configurations; however, these advantages require careful interfacial engineering to minimize recombination losses.

This paper adopts a performance-based analytical framework for evaluating perovskite solar cells (PSCs). Rather than merely listing fabrication methods and material compositions, each section critically examines how specific processes or components influence key operational metrics, including power conversion efficiency (PCE), charge transport behavior, thermal stability, and environmental durability. Issues such as hysteresis, lead toxicity, and ionic migration are not only identified but also discussed in relation to their underlying physical and chemical mechanisms. For instance, recombination losses at the perovskite/transport layer interface are examined using impedance spectroscopy models, whereas UV-induced degradation is addressed through compositional doping strategies. Where relevant, numerical data from recent experimental and simulation studies are included to support comparisons, such as efficiency improvements from 15.2% to 18.6% achieved using Ni-doped  $TiO_2$  as the Electron Transport Layer (ETL). This approach aligns the review with electrical and computer engineering perspectives by integrating modelling, diagnostic techniques, and real-time monitoring considerations.

## **2. Perovskite solar cell manufacturing**

In recent years, Perovskite Solar Cells (PSCs) have become one of the most exciting innovations in the solar energy sector. These next-generation solar cells have shown remarkable improvement in efficiency, increasing from just 3.8% in 2009 to 22.1% by 2016. This rapid progress places them alongside traditional silicon-based solar cells, but with the added advantages of lower cost, simpler processing, and greater flexibility. One of the most unique features of PSCs is their tunable bandgap, which allows them to be engineered to absorb different parts of the solar spectrum. This makes them highly adaptable for use in multi-junction cells and broad-spectrum light harvesting, allowing them to generate more electricity from sunlight than conventional materials.

A standout advantage of PSCs lies in their simple and cost-effective manufacturing process. Unlike silicon solar cells, which require high temperatures and complex machinery, perovskites can be processed using low-temperature, solution-based methods. These methods can produce ultrathin, lightweight, and flexible films, making PSCs ideal for portable solar panels, solar textiles, and building-integrated photovoltaics (BIPVs). Their potential for integration into glass windows, rooftops, walls, and even wearable gadgets makes them a highly versatile energy solution. The most commonly used fabrication technique at the lab scale is spin coating, where perovskite precursor solutions are dropped onto a spinning substrate, forming thin, uniform layers. Several promising methods have been developed to meet industrial demands. One of these is doctor-blade coating, a simple and scalable technique that spreads the perovskite solution evenly across a surface using a blade-like tool. This method has successfully produced PSCs with high uniformity and Power Conversion Efficiencies (PCEs) exceeding 15%, while being compatible with low-temperature, roll-to-roll processing.

Roll-to-Roll (R2R) manufacturing is another exciting development. It involves printing perovskite layers onto flexible substrates as they move through rollers, similar to how newspapers are printed. This method allows continuous production of large solar modules at high speed, making it ideal for commercial-scale fabrication. Combined with low-cost materials and rapid drying techniques, R2R can significantly reduce production time and costs, bringing us closer to widespread deployment of PSCs. Researchers are also experimenting with vapor-assisted deposition, slot-die coating, and spray coating, each offering unique benefits in terms of film quality, uniformity, and compatibility with various device structures. Some manufacturing systems, such as the MK-20 machine, have already demonstrated the ability to produce multiple PSC modules per hour with consistent quality, bridging the gap between laboratory research and real-world application. Looking ahead, the focus is not just on scaling up but also on improving material stability, device lifetime, and environmental friendliness. By combining advanced materials like nickel-doped  $\text{TiO}_2$ , carbon-based electrodes, and lead-free perovskite compositions, and integrating them with scalable manufacturing methods, researchers aim to create solar cells that are efficient, durable, and safe for mass deployment [16]. Perovskite solar cell manufacturing is evolving rapidly. With ongoing innovation in processing techniques and material engineering, PSCs are well-positioned to become a key player in the global transition to clean, affordable, and flexible solar energy solutions.

### *2.1. Analytical Overview of Manufacturing Techniques*

The manufacturing of PSCs has moved from lab-scale spin-coating toward scalable methods such as roll-to-roll (R2R) printing, doctor-blade coating, and inkjet deposition. Bin-Juine Huang et al. [21], The MK-20 system enables low-cost, continuous fabrication of perovskite solar cells with rapid heat

treatment for four layers. It coats 80 cm × 80 cm areas and produces six cells per hour, achieving 14.3% efficiency about 77% of that from smaller, lab-made cells. as shown in Figure 2.

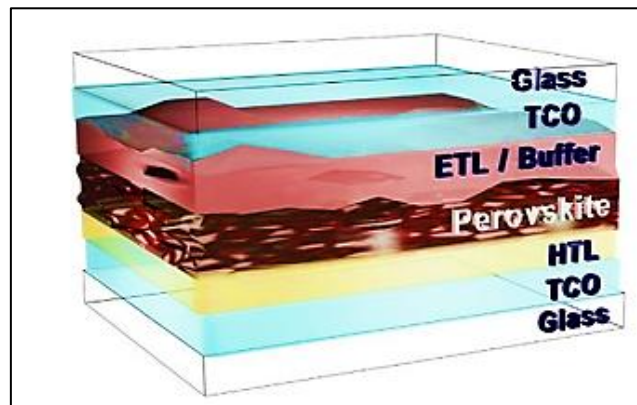


**Figure 2:** Perovskite cells are composed of four main parts [14].

Nathan L. Chang et al [17], examined roll-to-roll (R2R) production techniques, which offer the potential for high-throughput, low-cost perovskite solar module manufacture. They assessed two further optimized procedures and three R2R-compatible sequences. Important cost issues were found by their investigation, including transparent indium tin oxide (ITO) coatings, rear metal evaporation, and the high price of P3HT and PCBM materials. as depicted in Figure 3.

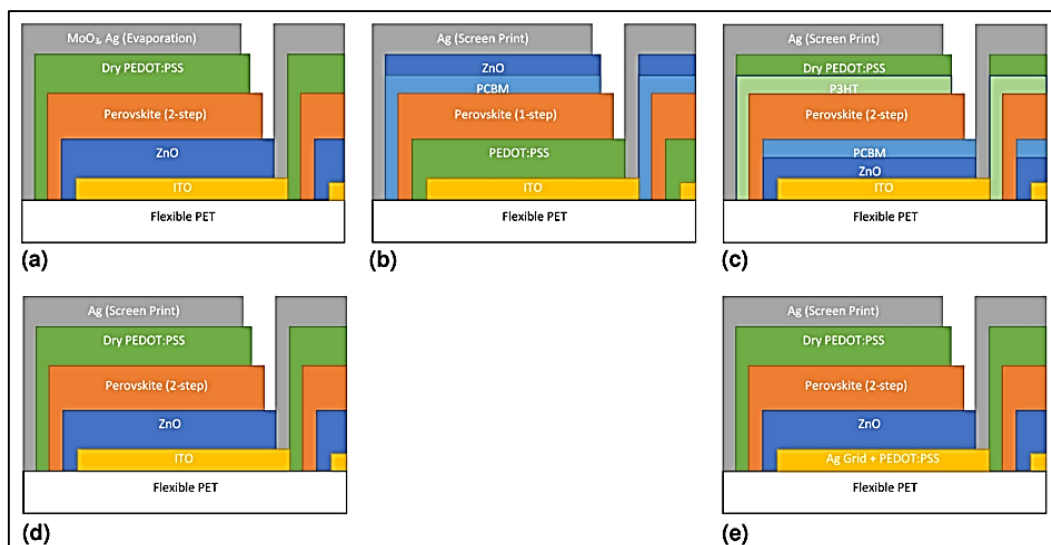


**Figure 3:** Different manufacturing processes [15].

Zhaoning Song et al. [18], carried out a thorough analysis of the parts and supplies utilized in the production of PSC modules. Glass substrates, wires, junction boxes, edge-sealing frames, lamination films, sealing agents, and interconnecting busbars are commonly found in these modules as depicted in Figure 4.

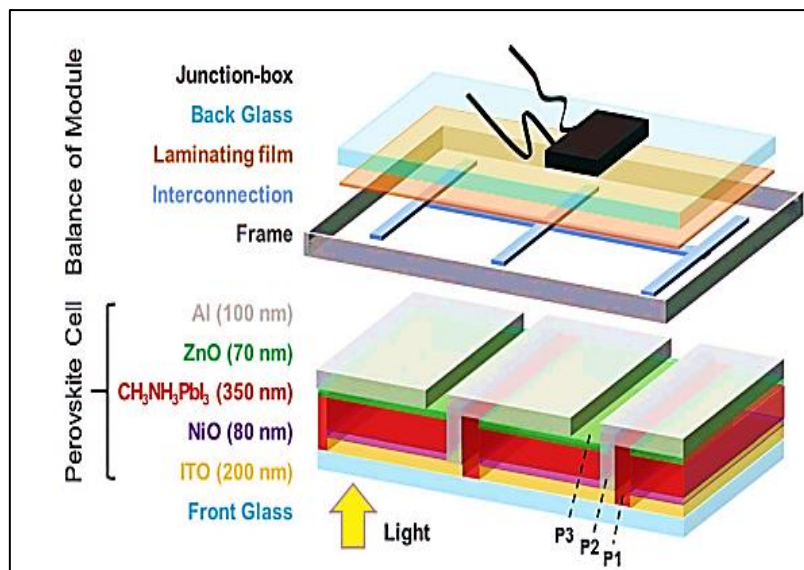


**Figure 4:** The module of perovskite solar cell [23]

Yuhei Ogomi et al. [19]. describe the photovoltaic capabilities of perovskite solar cells based on Sn/Pb halides that are all solid state. The composition of the cell is as follows: F-doped SnO<sub>2</sub> layered glass CH<sub>3</sub>NH<sub>3</sub>Sn<sub>x</sub>Pb<sub>(1-x)</sub>I<sub>3</sub> / regioregular poly (3-hexylthiophene-2,5-diyl) / compact titania layer/porous titania layer. Photovoltaic characteristics were not demonstrated by Sn halide perovskite itself. In SnI<sub>2</sub>, photovoltaic characteristics were noted upon the addition of PbI<sub>2</sub>. The CH<sub>3</sub>NH<sub>3</sub>Sn<sub>0.5</sub>Pb<sub>0.5</sub>I<sub>3</sub> perovskite demonstrated the best performance. With an open circuit voltage of 0.42 V, a fill factor of 0.50, and a short circuit current of 20.04 mA/cm<sup>2</sup>, an efficiency of 4.18% is recorded. The curve's edge representing the efficiency of incident photons to current. As shown in Fig. 5.

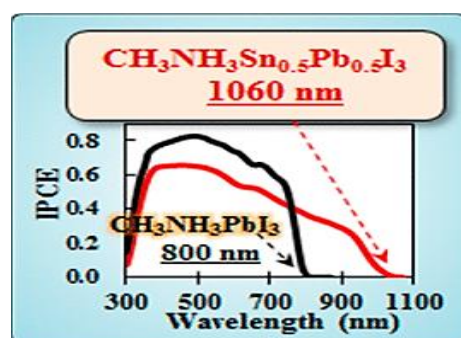


**Figure. 5.** Curve between Incident Photon Current Efficiency (IPCE) and that of CH<sub>3</sub>NH<sub>3</sub>PbI<sub>3</sub> perovskite solar cells [24]

Although spin-coating is widely used for its simplicity, its lack of film uniformity and process repeatability make it unsuitable for mass production. Conversely, doctor-blade and roll-to-roll (R2R) techniques have shown promise, achieving up to 14.3% module-level PCE. However, recent cost analyses highlight bottlenecks related to ITO electrodes and HTL materials like P3HT, suggesting a need for material substitution and deposition optimization.

### 3. Advanced structural in cell manufacturing

Since the emergence of perovskite solar cells (PSCs) based on dye-sensitized architectures, extensive research efforts have been directed toward improving device efficiency and long-term operational stability. Among the various factors contributing to this progress, the evolution of cell architecture has played a central role in enhancing photovoltaic performance.

#### 3.1 Mesoscopic structure of solid states

Khalid Mahmood et al. [20] were the first to investigate electro sprayed ZnO and Al-doped ZnO films as photoanodes for perovskite solar cells. In comparison with established thin-film deposition methods, including chemical vapor deposition and physical vapor deposition, electro spraying offered the advantages of a higher deposition rate and efficient film formation. The optimized pure ZnO film, with a thickness of 440 nm, achieved a power conversion efficiency (PCE) of 10.8%, mainly due to its high porosity, uniform morphology, and favorable electron transport characteristics. More importantly, Al doping further improved device performance, increasing the PCE from 10.8% to 12.0% and the open-circuit voltage from 1010 mV to 1045 mV. These improvements indicate that electro sprayed ZnO-based photoanodes possess strong potential for optoelectronic applications, particularly because the technique produces smooth films through the formation of relatively small and uniformly distributed droplets.

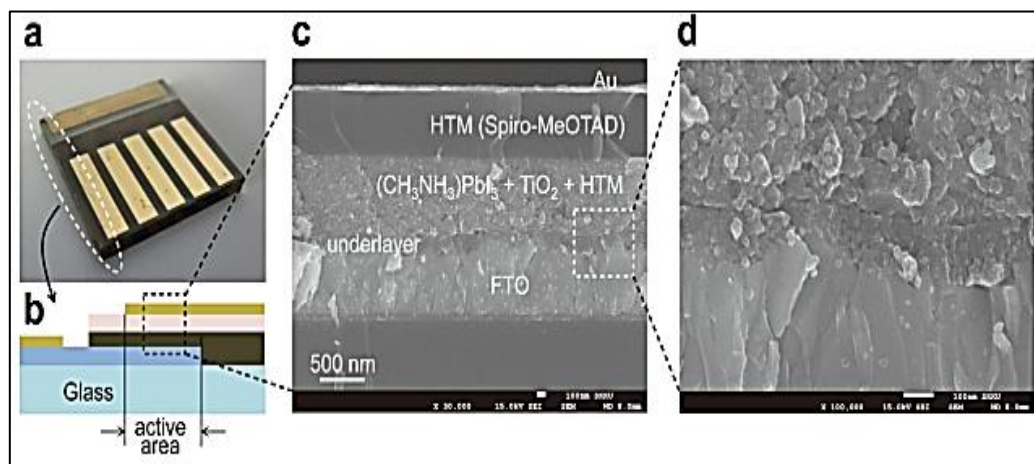


**Figure 6:** Shown, a. (An actual solid-state device), b. (device's cross-sectional structure), c. (cross-sectional SEM picture of the apparatus), d. (Interfacial connection structure of the active layer, underlayer, and FTO) [25].

#### 3.3 Intermediate superstructure and uniform framework

James M. Ball and co-workers reported that  $\text{CH}_3\text{NH}_3\text{PbI}_{3-x}\text{Cl}_x$  layers could still achieve efficiencies of up to 12.3% even when the annealing temperature was reduced to below  $150^\circ\text{C}$ . Under optimal conditions, ambipolar perovskite materials in planar film architectures also exhibited external quantum efficiencies exceeding 100%. In a related study, a mesoporous  $\text{TiO}_2/\text{CH}_3\text{NH}_3\text{PbI}_3$  hybrid incorporating a polymeric hole conductor, poly-triarylamine, achieved a power conversion efficiency

of 12.0%, together with improved open-circuit voltage and fill factor, demonstrating strong potential for the development of highly efficient solution-processed solar cells [21,22].

Cong-Cong Zhang et al. [23] introduced an external electric field (EEF)-assisted annealing strategy to enhance the photoelectric performance of planar organic-inorganic perovskite solar cells. This approach was found to strengthen the built-in electric field, thereby facilitating charge separation and transport, while also regulating the ion polarization orientation of the perovskite films to promote favorable crystallization. Compared with the conventional thermal-annealing-only process, the EEF-assisted treatment under an optimum up-EEF condition of 2.5 V/ $\mu\text{m}$  increased the power conversion efficiency from 15.33% to 17.26% for inverted PSCs and from 16.77% to 19.18% for conventional PSCs. These findings suggest that EEF-assisted annealing offers a promising strategy for improving perovskite film quality and overall device performance.

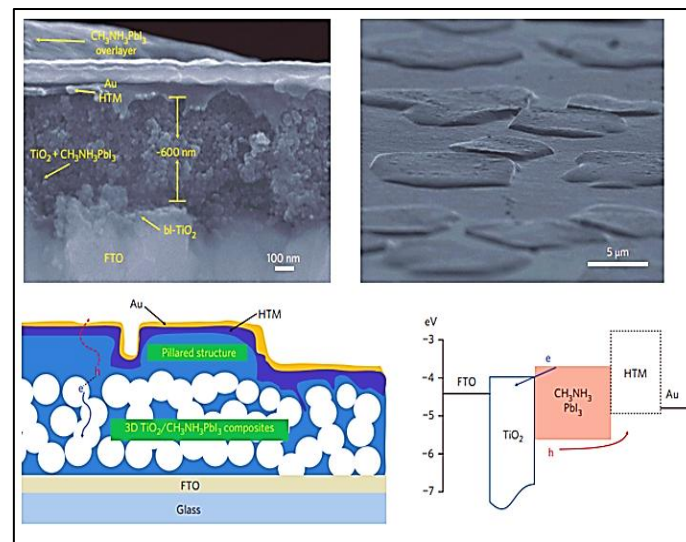


**Figure 7:** Shown typical layout and illustration of a cell's energy levels [22]

### 3.4 flat n-i-p variable frame

Yi Yang and co-workers introduced ammonium benzenesulfonate (ABS) into the perovskite precursor as a bifunctional additive for coordination and defect passivation. Photoluminescence (PL) and time-resolved PL mapping confirmed a significant reduction in trap density, which in turn suppressed non-radiative recombination and prolonged carrier lifetimes. As a result, the device achieved a peak power conversion efficiency (PCE) of 20.62%, mainly owing to improvements in the open-circuit voltage ( $V_{oc}$ ) and fill factor (FF). In addition, the unencapsulated cells exhibited remarkable stability, retaining 85% of their initial efficiency after 1400 hours under approximately 30% relative humidity [29].

Mustafa Haider and co-workers reported a power conversion efficiency of 12.1% for a planar PSC based on nickel phthalocyanine (NiPc). The device delivered an open-circuit voltage of 0.94 V, a short-circuit current density ( $J_{sc}$ ) of 17.64 mA/ $\text{cm}^2$ , and a fill factor of 73%, outperforming conventional devices employing copper phthalocyanine (CuPc), which is a commonly used metal phthalocyanine (MPc) [30]. As shown in Figure 8, the use of NiPc as the hole-transporting material contributed to improved device performance as shown in Figure 8.

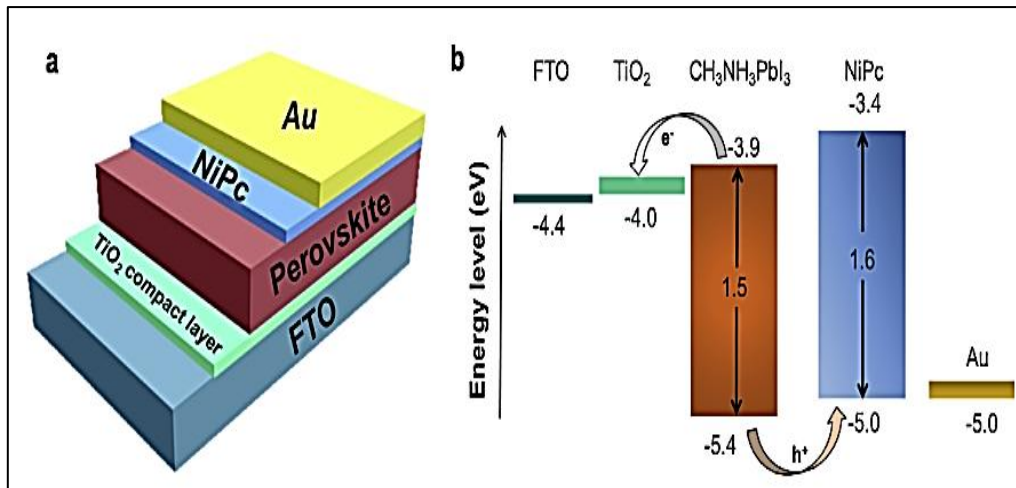


**Figure 8:** Diagram illustrating the device's energy levels and structure of the system [30]

Xingyue Liu et al. reported a carbon-based planar heterojunction perovskite solar cell (PSC) incorporating Ni-doped rutile  $\text{TiO}_2$  as the electron transport layer (ETL) and CuPc as the hole transport layer (HTL). The incorporation of nickel increased the Fermi level and improved charge-carrier mobility in the  $\text{TiO}_2$  layer, which in turn promoted more efficient charge extraction and transport. The optimized device, containing 0.01 M Ni, delivered a power conversion efficiency (PCE) of 17.46%. Moreover, the PSCs demonstrated excellent long-term stability, exhibiting no significant performance degradation after 1200 hours of storage under ambient conditions [31]. As illustrated in Figure 9, this study confirms the importance of ETL modification in improving both photovoltaic performance and device durability.

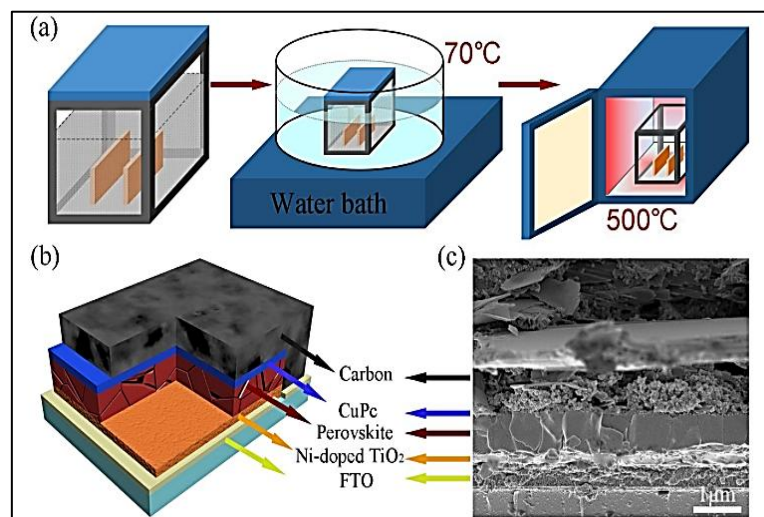


**Figure 9:** Diagram showing the solution-processed approach for manufacturing the Ni-doped  $\text{TiO}_2$  ETLs in perovskite solar cells [31]

### 3.5 flat p-i-n variable frame

Researchers adopted the inverted p-i-n structure from organic solar cells for perovskite devices, reversing the ETL and HTL layers. Docampo's team used a thin  $\text{CH}_3\text{NH}_3\text{PbI}_{3-x}\text{Cl}_x$  layer to achieve over 6% efficiency on flexible substrates and 10% on glass, proving perovskites' potential for low-cost, flexible solar technologies [32] as shown in Figure 10.

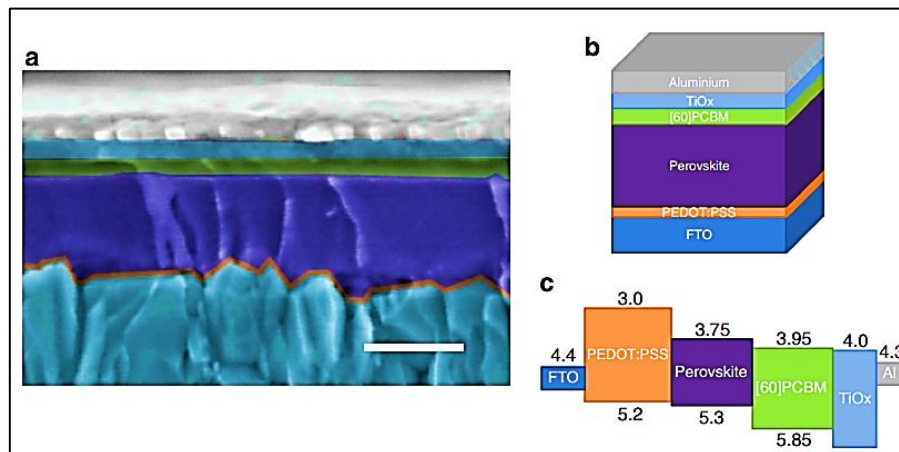


**Figure 10:** Scanning electron microscopy (SEM) cross-section; the scale bar is 250 nm. The various layers have been colored using the device schematic's color scheme and the approximate energy band diagram of the manufactured [32].

Jie Tang et al. developed highly crystalline nickel oxide (NiO) nanocrystals through an advanced solvothermal synthesis method. These nanocrystals, dispersed in toluene and stabilized with oleylamine ligands, were used to form high-quality HTLs via solution processing. The resulting PSCs demonstrated excellent performance, confirming the effectiveness of pre-synthesized NiO nanocrystals for scalable fabrication of efficient p-i-n devices [33] as shown in Figure 11.

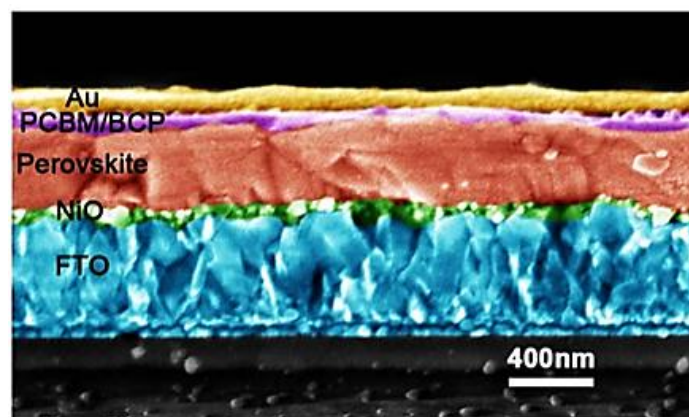


**Figure 11:** Shown the layers of perovskite solar cell [33].

Mesoscopic architectures, particularly those employing  $\text{TiO}_2$  scaffolds, have demonstrated improved charge collection efficiency; however, they remain susceptible to thermal instability. In contrast, inverted planar p-i-n structures offer simpler fabrication and better process compatibility, although they still face challenges related to interfacial compatibility. Comparative impedance analyses have shown that architecture-dependent recombination rates significantly influence the fill

factor (FF) and series resistance ( $R_s$ ), thereby underscoring the critical role of structural design in optimizing the electrical performance of perovskite solar cells.

#### 4. Operation of perovskite solar cells

Since their initial introduction in 2012, all-solid-state perovskite solar cells (PSCs) have attracted considerable attention because of their remarkable power conversion performance. Despite extensive research efforts, a complete understanding of their operational mechanisms is still evolving. Ravishankar et al. [34] provided important insights by showing that the open-circuit voltage ( $V_{oc}$ ) of PSCs is largely independent of the work function of the electron-selective layer.

Although organic solar cells (OSCs) and PSCs rely on different charge-generation mechanisms, they share similar material processing routes. This similarity has enabled fabrication strategies originally developed for OSCs to be adapted for PSC construction. Notably, PSCs have rapidly surpassed OSCs in terms of efficiency, highlighting their exceptional potential as a next-generation photovoltaic technology, as shown in Figure 12 [35].

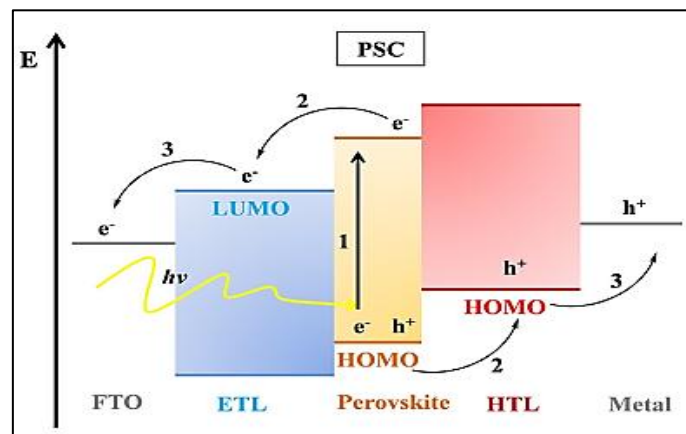


**Figure 12:** A diagram showing the basic processes in Perovskite solar cell (PSC), 1. generation of free charges and photon absorption, 2. Transport charge, 3. extraction of charges [35]

#### 5. Manufacturing Technique

Recent advances in perovskite solar cell (PSC) research have focused on optimizing both material compositions and fabrication strategies to enhance device performance and scalability. One notable development is the introduction of a mixed perovskite with a narrow bandgap,  $FA_{0.75}Cs_{0.25}Sn_{0.5}Pb_{0.5}I_3$ , which achieved an infrared absorption efficiency of 14.8%. By combining this material with a wider-bandgap perovskite,  $FA_{0.83}Cs_{0.17}Pb(I_{0.5}Br_{0.5})_3$ , researchers successfully constructed a mechanically stacked four-terminal tandem device with an overall efficiency of 20.3%. Unlike many other Sn-based perovskites, this material system also demonstrated excellent thermal and environmental stability [36], as shown in Figure 13.

David T. Moore and co-workers examined the effect of lead salt chemistry, including iodide, acetate, nitrate, and chloride precursors, on the crystallization kinetics of perovskite films using in-situ X-ray scattering. Their findings revealed that lead salt selection has a decisive influence on film formation and crystal-growth behavior, thereby strongly affecting the structural quality and photovoltaic performance of the resulting devices [37].

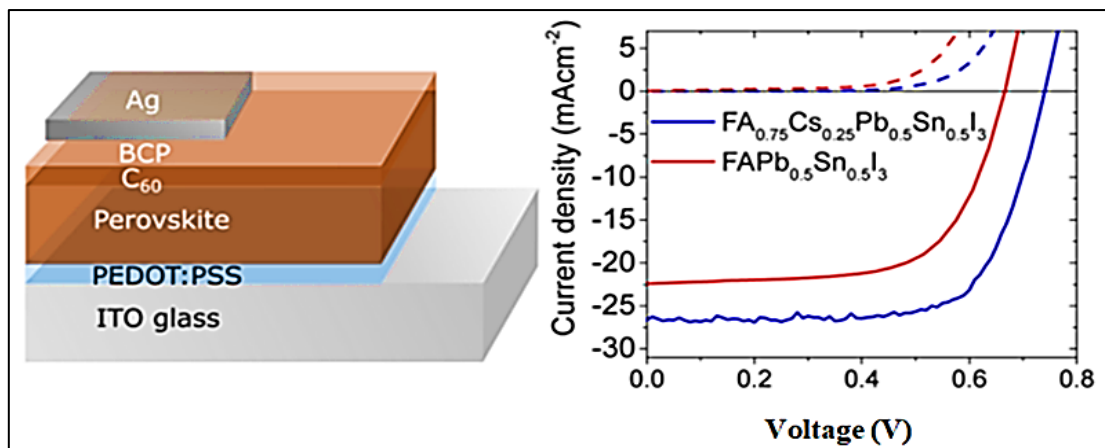


**Figure 13:** Diagram illustrating perovskite solar cell device design. With a diagram showing the relationship between current density (mA/cm<sup>2</sup>) & voltage (V) [36]

In a related development, Nam Joong Jeon et al. designed a bilayer perovskite solar cell (PSC) architecture that integrated both planar and mesoscopic characteristics through a fully solution-processed route. The absorber layer consisted of  $\text{CH}_3\text{NH}_3\text{Pb}(\text{I}_{1-x}\text{Br}_x)_3$  of  $x = 0.1-0.15$ , while poly(triarylamine) was employed as the hole-transport material. Through solvent engineering and the formation of a  $\text{CH}_3\text{NH}_3\text{I}-\text{PbI}_2-\text{DMSO}$  intermediate phase, assisted by toluene drop-casting, they achieved a dense and highly uniform perovskite film, resulting in a certified power conversion efficiency of 16.2% with negligible hysteresis [38].

Further optimization through compositional tuning, particularly by incorporating  $\text{MAPbBr}_3$  into  $\text{FAPbI}_3$ , improved phase stability and increased the device efficiency to above 18% under standard solar illumination. Collectively, these results highlight the compositional versatility and significant promise of hybrid lead halide perovskites for the development of high-performance photovoltaic devices [39], as illustrated in Figure 14.

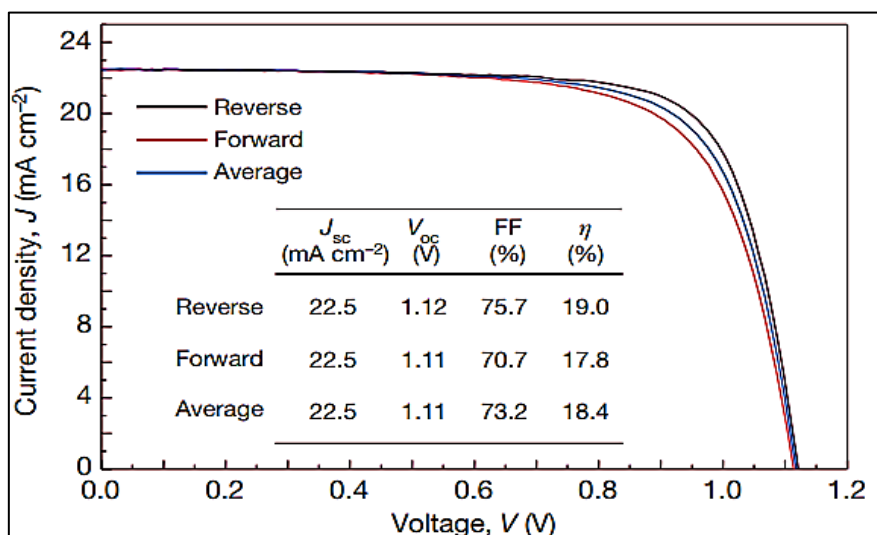


**Figure 14:** A diagram, curves between Voltage and Current density [39]

Further improvements were achieved by delaying  $\text{PbI}_2$  crystallization during the sequential deposition process, which enabled the fabrication of reproducible planar perovskite solar cells (PSCs)

with average efficiencies of 12.5% and peak efficiencies of 13.5% [40]. In another notable development, a fully printable mesoscopic PSC was fabricated by infiltrating a double layer of mesoporous  $\text{TiO}_2$  and  $\text{ZrO}_2$  with a perovskite precursor solution containing  $\text{PbI}_2$ , MAI, and 5-AVA iodide. The incorporation of the 5-AVA additive enhanced pore filling and improved crystal interaction, resulting in a stable device with an efficiency of 12.8%, which retained its performance for more than 1000 hours under ambient air conditions [41], as shown in Figure 15.

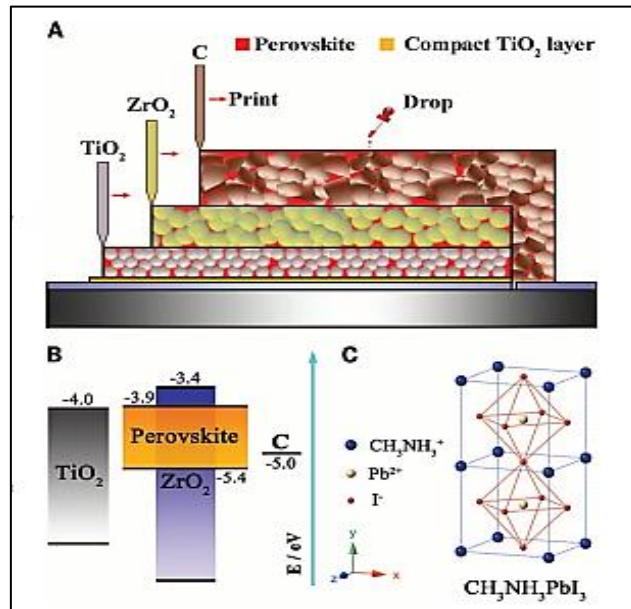


**Figure 15:** A diagram that illustrates the triple-layer perovskites cross section, B. The triple-layer device's energy band diagram, C. The perovskite  $\text{MAPbI}_3$  crystal structure [41].

Power conversion efficiencies of up to 15.1% have been reported through the use of specialized hole-transporting layers, highlighting the importance of interfacial engineering in improving PSC performance. Doctor-blade coating has attracted considerable interest as a solution-based thin-film deposition technique because of its low processing temperature, low cost, and excellent scalability. Its compatibility with high-throughput roll-to-roll fabrication also makes it highly promising to produce large-area PSC devices [42].

Hsieh et al. [43] further showed that  $\text{TiO}_2$  deposition via ultrasonic spray pyrolysis (USP) effectively reduced interfacial resistance, resulting in an increase in power conversion efficiency from 12.98% to 16.13% relative to conventional sol-gel deposition.

Beyond materials and fabrication, recent developments have also emphasized intelligent monitoring and control of PSC systems. The incorporation of ESP8266-based microcontrollers with cloud platforms such as Ubidots has enabled real-time monitoring of key module parameters, including temperature, irradiance, and current-voltage (I-V) characteristics. Such integration supports predictive fault diagnosis and adaptive energy optimization, which are increasingly important for smart energy applications. Furthermore, embedded control algorithms enable dynamic maximum power point tracking (MPPT), thereby enhancing power extraction under variable irradiance conditions.

At the same time, electrical modeling and diagnostic techniques, such as I-V characterization, external quantum efficiency (EQE) analysis, and impedance spectroscopy, have become essential for understanding the internal operation of PSCs. Nyquist and Bode analyses, for example, allow the identification of characteristic time constants associated with dielectric relaxation and charge-

transfer processes. In addition, the extraction of parameters such as series resistance ( $R_s$ ), shunt resistance ( $R_{sh}$ ), and carrier lifetime facilitates circuit-level simulation and SPICE-based model development. Collectively, these methodologies reinforce the growing importance of electrical engineering approaches in the analysis and optimization of perovskite solar technologies.

## 6. Summary of Literature Review

Following the discussion of the manufacturing processes and operational mechanisms of perovskite solar cells, Table 1 summarizes the detailed photovoltaic parameters of PSCs reported in the literature. The table includes the types of materials used in PSC fabrication, together with key performance metrics such as power conversion efficiency, open-circuit voltage, short-circuit current density, and fill factor. The primary objective of this table is to review and compare these important photovoltaic parameters across different material systems and device architectures.

**Table 1:** Detailed photovoltaic parameters of PSCs

Power conversion efficiency) PCE)	open-circuit voltage ( $V_{oc}$ )	short circuit current density ( $J_{sc}$ )	fill factor (FF)	Configuring a Device	Year	Reference
6.54	0.706	15.82	0.586	Pt/Liquid Electrolyte /CH <sub>3</sub> NH <sub>3</sub> PbI <sub>3</sub> (QD) / TiO <sub>2</sub> /FTO	2011	[44]
9.7	0.888	17	0.62	Au/spiro OMeTAD/ CH <sub>3</sub> NH <sub>3</sub> PbI <sub>3</sub> / mTiO <sub>2</sub> /FTO	2012	[45]
17.01	1.056	21.64	0.741	Au/spiro-MeOTAD/ Cuboid MAPbI <sub>3</sub> / MAPbI <sub>3</sub> / m-TiO <sub>2</sub> /c-TiO <sub>2</sub> /FTO	2024	[46]
19.3	1.114	23	0.74	Au/Spiro-OMeTAD/ Perovskite/m-Li:TiO <sub>2</sub> / Perovskite/ FTO	2014	[47]
20.2	1.06	24.7	0.775	Au/PTAA /Perovskite /(bl/m-TiO <sub>2</sub> )/FTO	2015	[48]

**Table 1:** Detailed photovoltaic parameters of PSCs (Cont.)

Power conversion efficiency) PCE)	open-circuit voltage ( $V_{oc}$ )	short circuit current density ( $J_{sc}$ )	fill factor (FF)	Configuring a Device	Year	Reference
6.54	0.706	15.82	0.586	Pt/Liquid Electolyte /CH <sub>3</sub> NH <sub>3</sub> PbI <sub>3</sub> (QD) / TiO <sub>2</sub> /FTO	2011	[44]
9.7	0.888	17	0.62	Au/spiro OMeTAD/ CH <sub>3</sub> NH <sub>3</sub> PbI <sub>3</sub> / mTiO <sub>2</sub> /FTO	2012	[45]
17.01	1.056	21.64	0.741	Au/spiro-MeOTAD/ Cuboid MAPbI <sub>3</sub> / MAPbI <sub>3</sub> / m-TiO <sub>2</sub> /c-TiO <sub>2</sub> /FTO	2024	[46]
19.3	1.114	23	0.74	Au/Spiro-OMeTAD/ Perovskite/m-Li:TiO <sub>2</sub> / Perovskite/ FTO	2014	[47]
20.2	1.06	24.7	0.775	Au/PTAA /Perovskite /(bl/m-TiO <sub>2</sub> ) /FTO	2015	[48]

**Table 2:** Cost Comparison Between Perovskite Solar Cells and Conventional Photovoltaic Technologies

Type of Solar Cell	Manufacturing Cost (USD/W)	Efficiency (%)	Material Cost	LCOE (USD/kWh)	Scalability	Key Advantages	Reference
Perovskite Single-Junction	0.21 – 0.28	17 – 22	Low	0.03 – 0.05	High (emerging)	Low cost, lightweight, easy to process	[51]
Perovskite-Silicon Tandem	0.29 – 0.42	25 – 35	Medium	0.025 – 0.04	Moderate to High	Higher efficiency, compatible with silicon tech	[52] [53]
Crystalline Silicon (c-Si)	0.25 – 0.27	18 – 22	Medium	0.035 – 0.045	Very High	Proven tech, long lifespan, mature supply chain	[54],[55]
Advanced Silicon (PERC)	~0.285	20 – 23	Medium	0.03 – 0.04	Very High	High efficiency, available infrastructure	[54],[55]

In recent years, increasing interest among universities and developing nations in small satellite missions has generated a growing demand for photovoltaic emulators in solar-cell subsystem testing. These emulators allow the performance of solar-cell systems to be evaluated under a range of space-related environmental conditions. Their importance lies in their versatility, particularly their capability to simulate different solar-cell technologies used in space applications.

Furthermore, accurate prediction of solar radiation is essential for various renewable energy applications. A wide range of methods, including artificial intelligence-based and hybrid approaches, has been applied for daily solar-radiation estimation. Among these, the Gaussian Process Regression (GPR) algorithm has recently demonstrated promising performance in fields such as remote sensing and Earth science [56][57].

## 7. Result and Discussion

Perovskite solar cells are experiencing rapid progress in both performance and efficiency, supported by low-cost manufacturing techniques that enhance their commercial scalability. Advanced electron transport materials and structural modifications, such as corrugations, metal-alloy incorporation, and chemical additives, have played a crucial role in improving device efficiency and stability. Nevertheless, major challenges remain, particularly in relation to long-term stability and lead toxicity. Looking forward, the integration of PSCs with tandem cell technologies and the development of lead-free perovskite systems are likely to define the future direction of this technology in the global solar energy market.

Table 3 demonstrates that material selection significantly influences PSC efficiency. Conventional  $\text{CH}_3\text{NH}_3\text{PbI}_3$ -based systems generally show moderate performance, whereas doped and tandem configurations can achieve power conversion efficiencies above 17-20%, reflecting the rapid advancement and ongoing optimization of perovskite-based materials. This overall trend is also illustrated in Figure 16.

**Table 3: Power Conversion Efficiency (PCE) of Different PSC Materials**

Material Composition	Architecture	Efficiency (%)	Voc (V)	Reference
CH <sub>3</sub> NH <sub>3</sub> PbI <sub>3</sub>	TiO <sub>2</sub> / CH <sub>3</sub> NH <sub>3</sub> PbI <sub>3</sub> / Electrolyte / Pt	3.81	0.61	[4]
CH <sub>3</sub> NH <sub>3</sub> PbI <sub>3</sub> (QD)	TiO <sub>2</sub> / Liquid Electrolyte / Pt	6.54	0.706	[48]
MAPbI <sub>3</sub>	Mesoporous TiO <sub>2</sub> / spiro- MeOTAD	9.7	0.888	[49]
ZnO-based PSC	ZnO / MAPbI <sub>3</sub>	10.8	-	[19]
Ni-doped TiO <sub>2</sub> / MAPbI <sub>3</sub>	Carbon-based planar	17.46	-	[25]
Perovskite- perovskite tandem	Four-terminal stacked	20.3	-	[32]

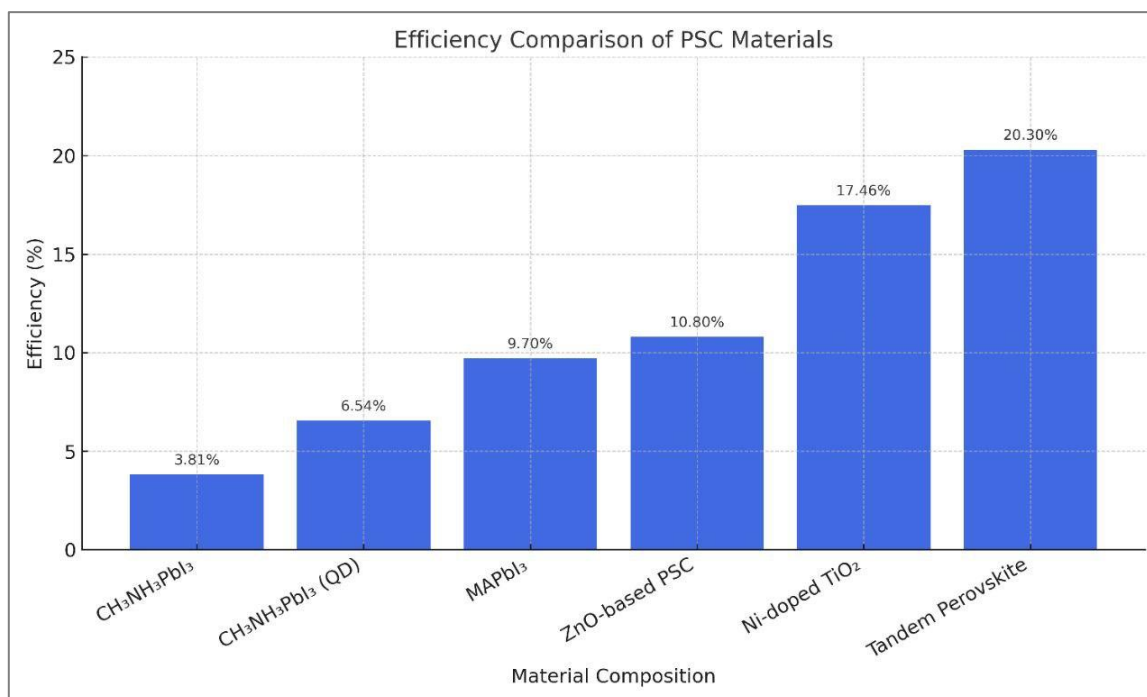
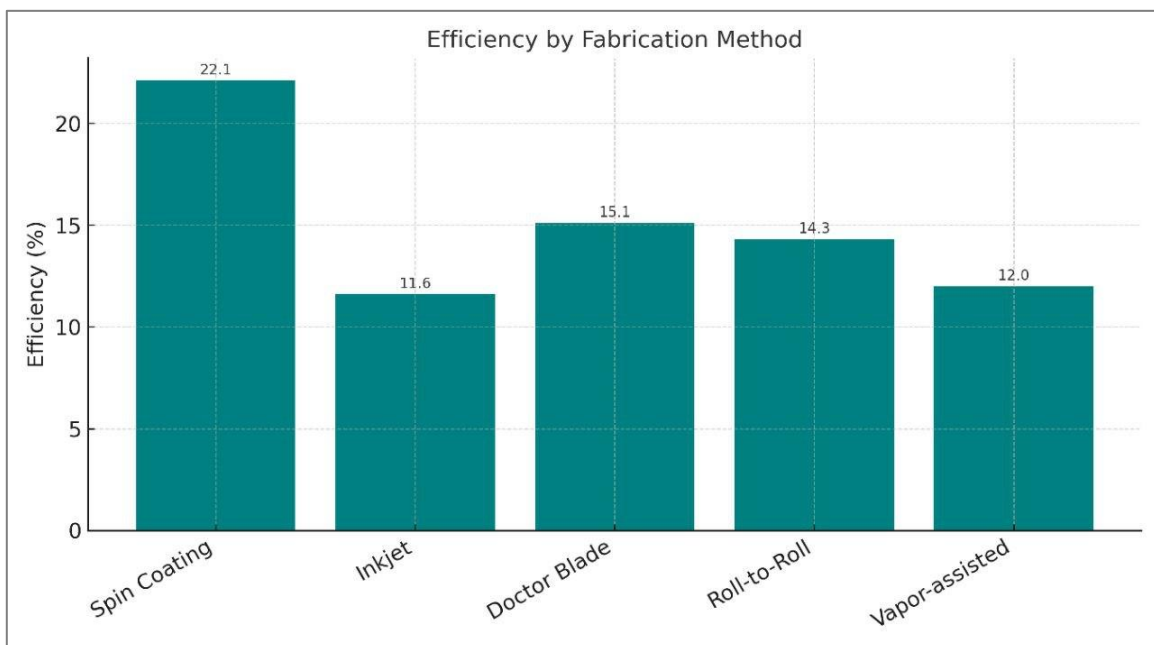


**Figure 16:** A diagram to the efficiency comparison of PSC Materials

Table 4 indicates that, among the various fabrication techniques, roll-to-roll and doctor-blade coating are the most promising for industrial-scale production because of their scalability and relatively low cost. In contrast, spin coating continues to dominate laboratory-based research owing to its simplicity and effectiveness in producing uniform films. The key challenge, however, lies in translating these high-efficiency laboratory methods into scalable manufacturing processes without significant deterioration in device performance. This trend is further illustrated in Figure 17.

**Table 4: Comparison of Fabrication Methods for PSCs**

Method	Scalability	Cost Level	Temperature Requirement	Efficiency Achieved
Spin Coating	Low	Low	Low	Up to 22.1%
Inkjet Printing	Medium	Low	Moderate	11.6%
Doctor Blade Coating	High	Very Low	Low	15.1%
Roll-to-Roll	Very High	Low	Low	14.3% (MK-20)
Vapor-assisted Deposition	Medium	Medium	High	>12%



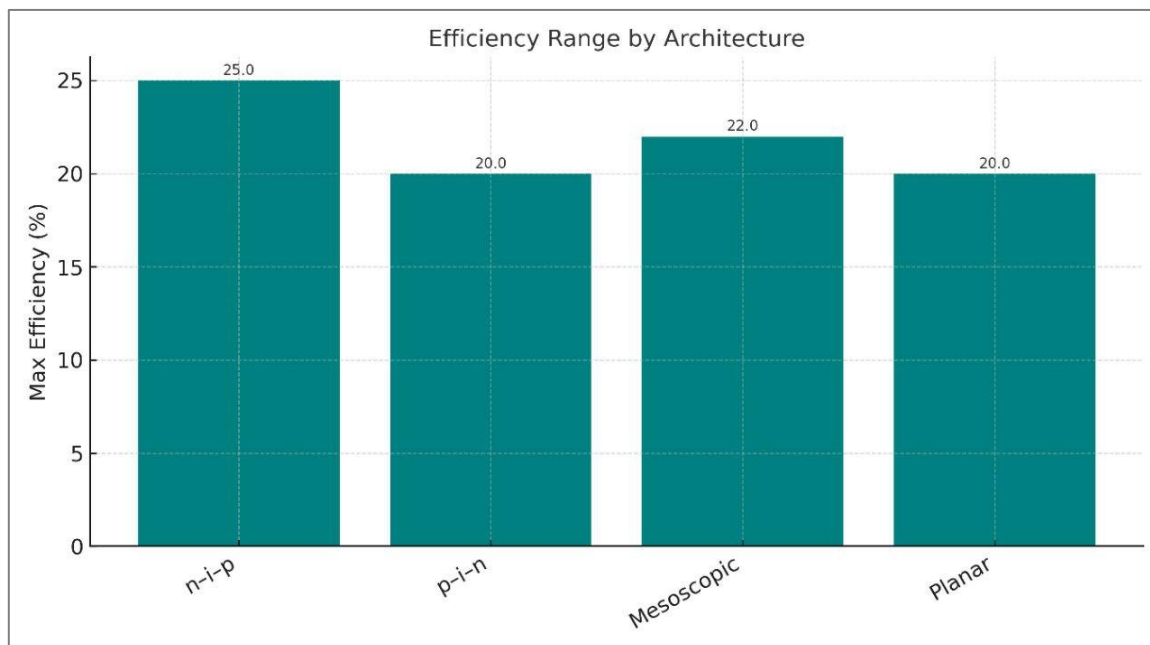
**Figure 17:** A diagram to the Comparison of Fabrication Methods for PSCs

Table 5 shows that cell architecture has a significant influence on charge transport behavior and overall device efficiency. The conventional n-i-p configuration remains the most widely adopted architecture, whereas inverted p-i-n structures offer advantages in terms of mechanical flexibility and processing compatibility. Mesoscopic architectures generally improve charge separation and carrier

collection, while planar structures are often preferred because of their simpler fabrication process. These comparative trends are further illustrated in Figure 18.

**Table 5: Comparison of PSC Architectures and Their Impact on Performance**

Architecture	Charge Transport Mechanism	Typical Efficiency Range (%)	Advantages
n-i-p (Normal)	Electron first, hole second	15–25%	High efficiency, widely studied
p-i-n (Inverted)	Hole first, electron second	10–20%	Low-temperature processing, flexibility
Mesoscopic	Hybrid conduction via porous TiO <sub>2</sub>	12–22%	High surface area, improved stability
Planar	Direct conduction through flat layers	10–20%	Simple structure, easy to fabricate



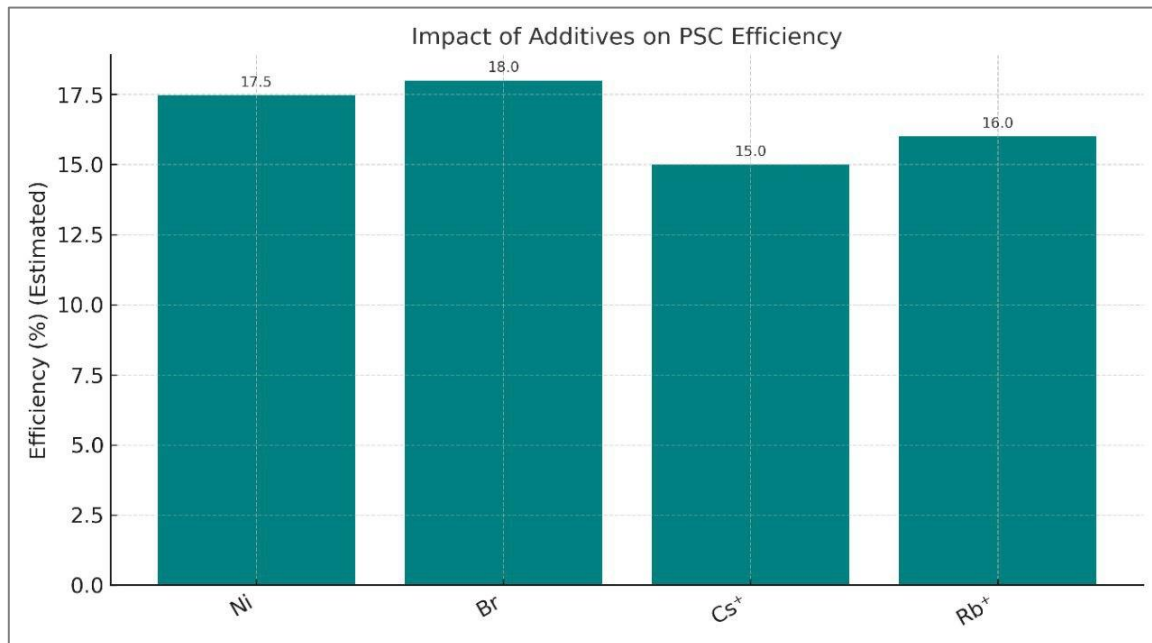
**Figure 18:** A diagram to the Comparison of PSC Architectures and Their Impact on Performance

Table 6 highlights the importance of additives and compositional tuning in enhancing the performance of perovskite solar cells (PSCs). Elements such as Ni, Br, Cs, and Rb play critical roles in improving charge transport, structural stability, and long-term device durability, thereby contributing significantly to the commercial viability of PSC technology. These effects are further illustrated in Figure 19. In Table 7, Perovskite-silicon tandem cells may surpass silicon in efficiency, but long-term stability and mass production are still under development, as shown in Figure 20.

Compositional engineering of perovskite absorber materials has enabled substantial improvements in both device performance and environmental stability. For example, the incorporation of Br<sup>-</sup> or Cs<sup>+</sup> into the CH<sub>3</sub>NH<sub>3</sub>PbI<sub>3</sub> matrix has been shown to enhance phase stability and improve band alignment. Similarly, Ni-doped TiO<sub>2</sub> electron transport layers (ETLs) have been reported to increase the power conversion efficiency from 15.2% to 17.46% while maintaining ambient stability for more than 1200 hours. Nevertheless, such modifications must also be assessed in terms of environmental impact and cost-effectiveness to ensure their practical viability for large-scale application.

**Table 6:** Effect of Additives and Composition on PSC Performance

Additive/Element	Functionality	Performance Impact	Reference
Ni Doping	Improves electron mobility	Raised PCE to 17.46%	[25]
Br Inclusion	Widen bandgap and improve stability	Over 18% with phase control	[36]
Cs <sup>+</sup> Ions	Enhance moisture stability	Improved long-term stability	[42]
Rb <sup>+</sup> Ions	Passivate defects	Stabilized structure in humidity	[42]



**Figure 19:** A diagram to the Effect of Additives and Composition on PSC Performance

In table (7) Perovskite-silicon tandem cells may surpass silicon in efficiency, but long-term stability and mass production are still under development. As shown in figure (20).

**Table 7: PSCs vs. Silicon Solar Cells**

Technology	Efficiency	Cost	Stability	Scalability
Mono-Si	22–26%	High	>25 years	High
Poly-Si	17–22%	Medium	>20 years	High
PSC (Lab-scale)	Up to 25.7%	Low	<5 years	Low
Tandem PSC	26–29%	Medium	5–10 years	Medium
PSC–Si Tandem	29–33%	High	>10 years	Emerging

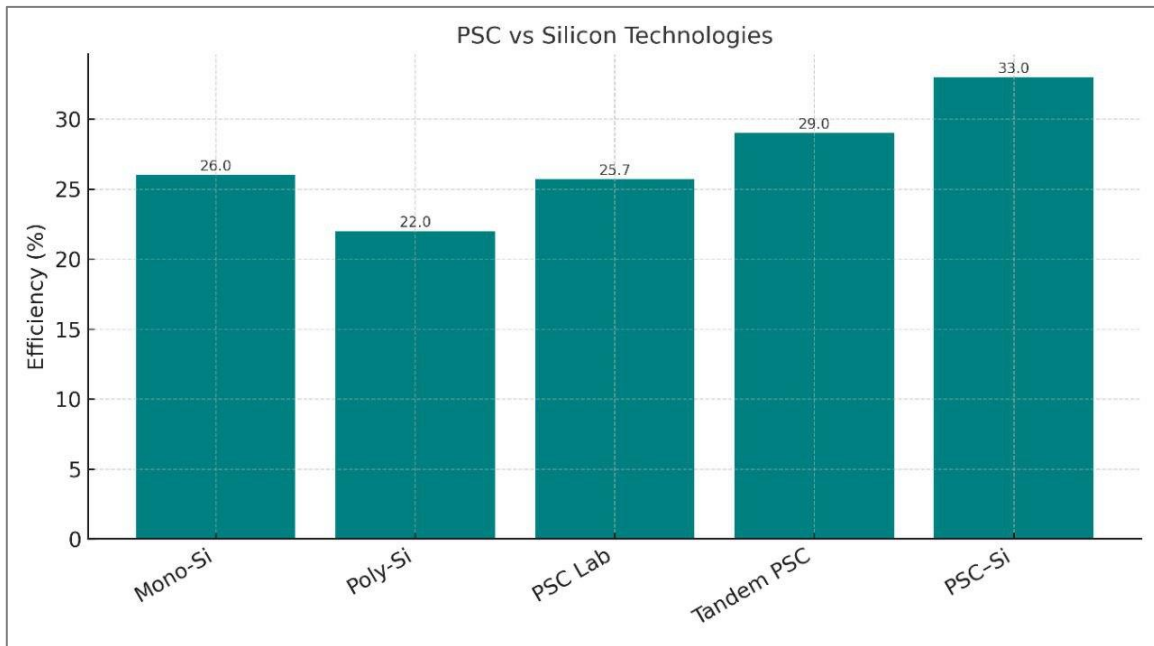


**Figure 20:** A diagram PSCs vs. Silicon Solar Cells

In Table 8, the versatility of PSCs makes them ideal for next-generation applications, especially in portable, flexible, and aesthetic energy solutions.as shown in Figure 21.

**Table 8:** Applications of Perovskite Solar Cells

Application	Form Factor	Advantages	Challenges
Wearables	Flexible films	Lightweight, bendable	Mechanical stress
Building-integrated	Transparent panels	Aesthetic integration	Weather exposure
Portable Chargers	Foldable modules	High mobility	Limited output
Agrivoltaics	Semi-transparent	Dual land use	Light absorption loss
Space Applications	Ultralight panels	High efficiency	Radiation exposure

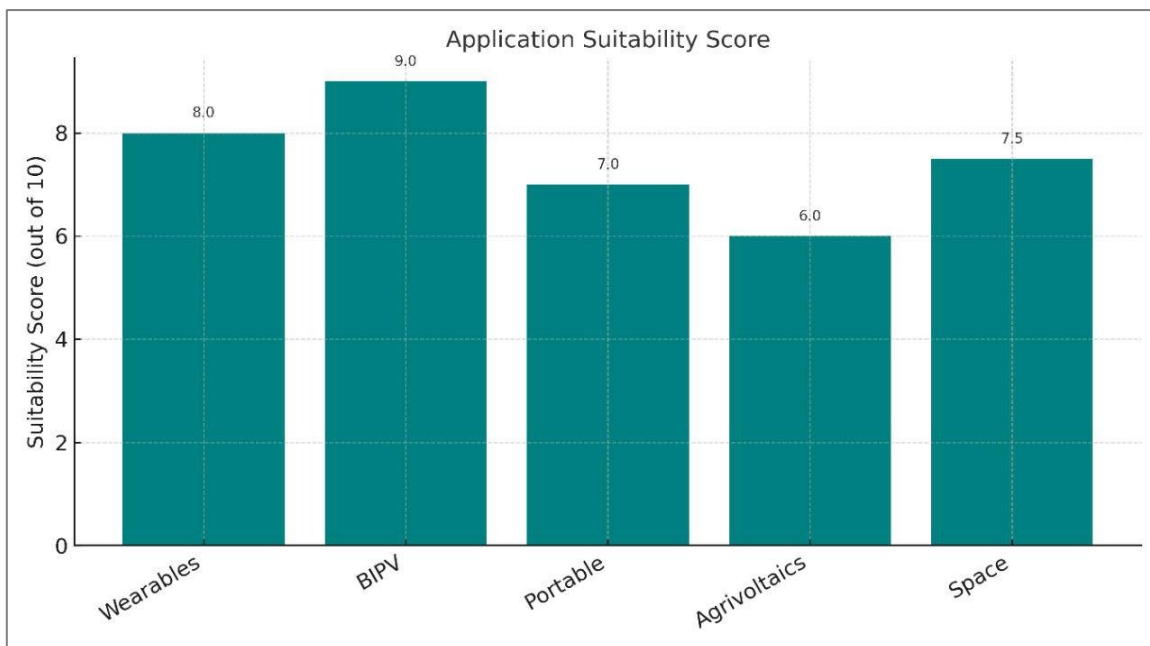


**Figure 21:** A shown diagram Applications of Perovskite Solar Cells

The diagram below compares the efficiencies of different perovskite solar cells (PSCs), particularly between  $\text{CH}_3\text{NH}_3\text{PbI}_3$ -based devices and doped or double-doped compounds, including tandem PSCs. It illustrates the significant progress achieved in the photovoltaic conversion efficiencies of perovskite materials in recent years, as shown in Figure 22.

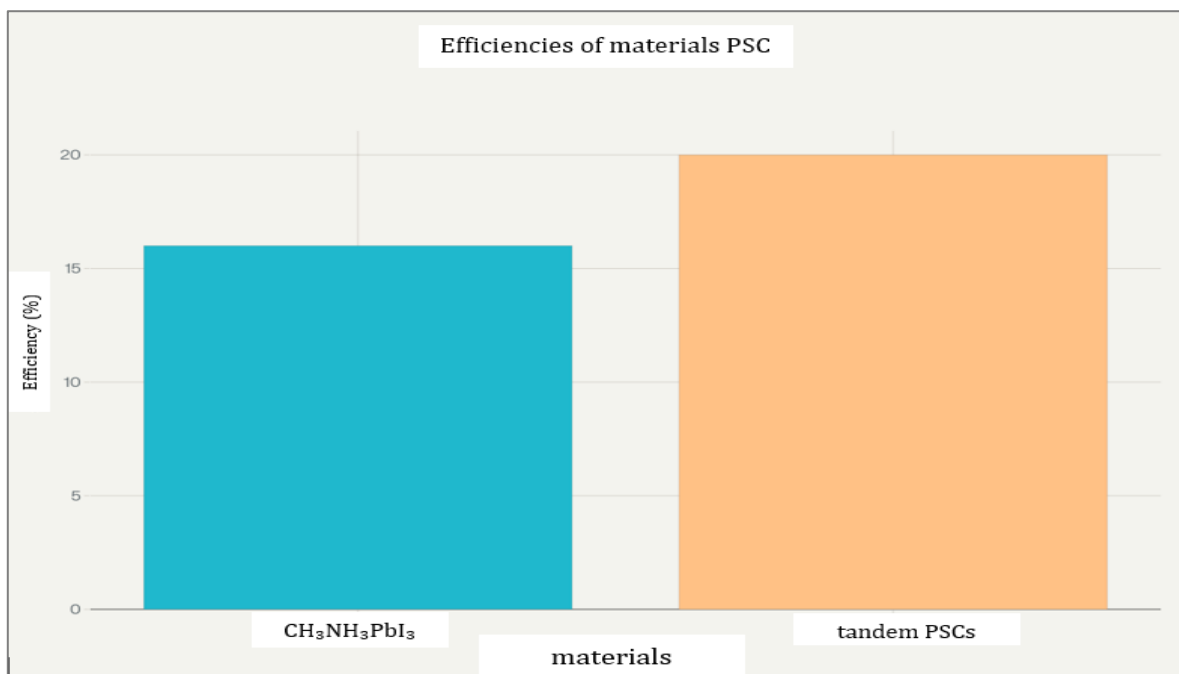


**Figure 22:** A diagram Comparison between  $\text{CH}_3\text{NH}_3\text{PbI}_3$  and tandem or binary compounds (Tandem PSC)

Figure 23 presents a detailed comparison of different perovskite solar cell (PSC) architectures, including n-i-p, p-i-n, mesoscopic, and planar configurations, in terms of charge collection efficiency, ease of fabrication, and structural flexibility. The figure highlights the relative strengths and limitations of these four major design approaches based on three critical performance and manufacturing criteria. The analysis are:

### 1. Charge Collection Efficiency

The n-i-p and mesoscopic architectures exhibited the highest charge collection efficiency, indicating superior performance in charge extraction and transport. This advantage is generally attributed to their optimized layer configurations, which facilitate the efficient separation and collection of photogenerated charge carriers. In contrast, the p-i-n and planar structures showed slightly lower performance, suggesting that although their charge collection remains effective, it is somewhat limited by their simpler architectures or by differences in material selection that may influence extraction efficiency.

### 2. Fabrication Ease

The p-i-n and planar architectures demonstrated the greatest ease of fabrication. Their relatively simple structures are more compatible with scalable manufacturing processes, which can reduce production cost and improve reproducibility. The n-i-p architecture showed a moderate level of fabrication ease, indicating that although its processing is manageable, it generally involves additional steps or tighter process control. By comparison, the mesoscopic design ranked lowest in this category, primarily because it requires the formation of a mesoporous scaffold, which introduces greater structural complexity and demands more specialized processing conditions.

### 3. Flexibility

The p-i-n and planar architectures also showed the highest degree of flexibility. Their compatibility with flexible substrates makes them particularly suitable for applications such as wearable electronics and other bendable photovoltaic devices. The mesoscopic architecture exhibited moderate flexibility, reflecting a balance between structural robustness and mechanical adaptability. In contrast, the n-i-p design showed the lowest flexibility, which is likely associated with its reliance on higher processing temperatures or rigid materials that are less suitable for flexible applications.

Key Findings show that the comparison indicates that n-i-p and mesoscopic architectures are more favorable when high electrical performance, particularly charge collection efficiency, is the primary objective. In contrast, p-i-n and planar architectures are more attractive for large-scale manufacturing and flexible-device applications because of their simpler processing requirements and better compatibility with flexible substrates. These observations suggest that there is no universally optimal PSC architecture. Instead, the selection of device design depends strongly on the intended application. Architectures such as n-i-p and mesoscopic structures are more suitable for achieving high photovoltaic performance, although they may involve greater fabrication complexity and cost. On the other hand, p-i-n and planar configurations are better suited for scalable production and flexible applications.

Meanwhile, the technical Significance comparison highlights the need to balance electrical performance, manufacturability, and mechanical flexibility in the development of PSC technology. The choice of the most appropriate architecture should therefore be guided by the intended end use, whether the priority is maximum efficiency, structural flexibility, or low-cost mass production. Future

research is expected to focus not only on improving material properties but also on refining device architectures to overcome the current limitations associated with each design approach.

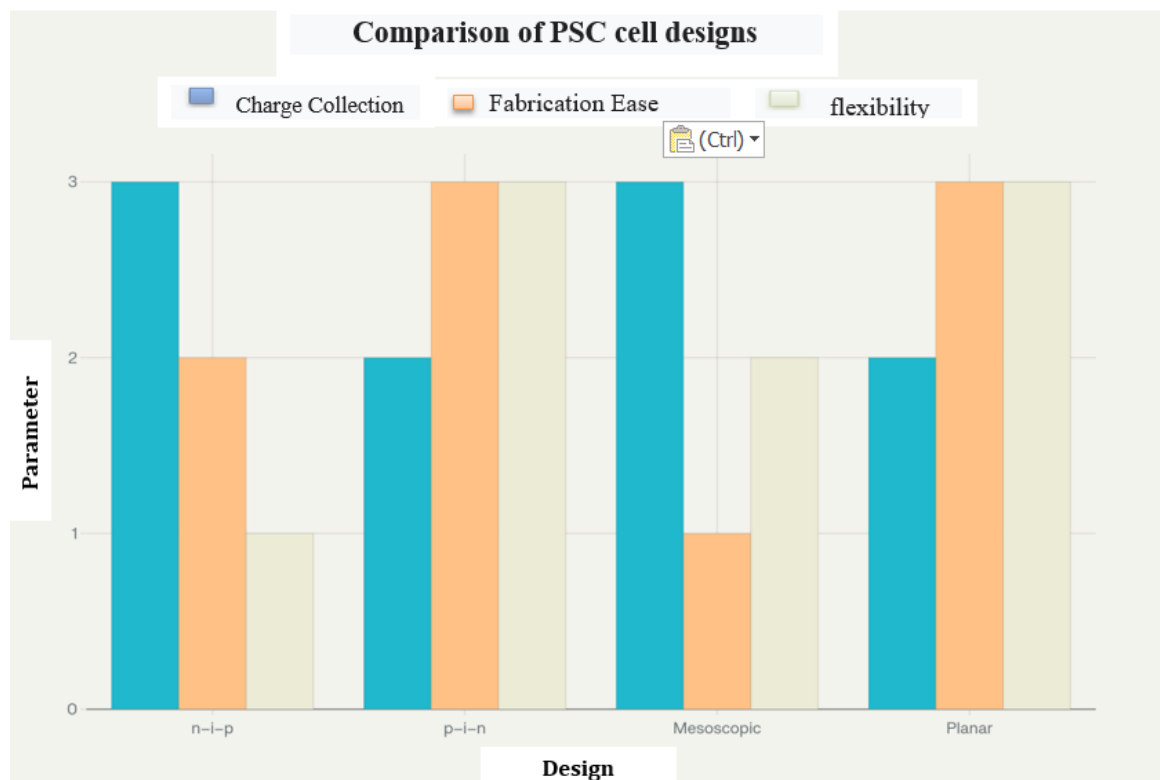


**Figure 23:** A diagram Comparison of PSC cell designs and their impact

Although perovskite solar cells (PSCs) have demonstrated remarkable success at the laboratory scale, their practical deployment is still hindered by major challenges, particularly lead toxicity, operational instability under UV irradiation and moisture exposure, and the complexities of scalable manufacturing. Lead-free alternatives based on tin and bismuth have attracted increasing attention as safer material systems, yet their efficiencies still remain below 10%, limiting their immediate competitiveness. At the same time, hybrid tandem architectures, especially PSC/Si devices, have surpassed 30% efficiency, highlighting their strong commercial potential. Nevertheless, these systems must still overcome challenges related to cost parity and thermal-cycling durability in order to meet the requirements for grid-scale implementation. Therefore, advanced encapsulation technologies and 2D/3D perovskite blend engineering are emerging as critical strategies for enhancing the long-term stability and reliability of PSC technology.

### 8. Conclusion

Perovskite solar cells (PSCs) have emerged as one of the most promising photovoltaic technologies of the 21st century, demonstrating an extraordinary rise in power conversion efficiency from 3.8% to over 25% in just over a decade. This remarkable progress highlights the strong potential of PSCs as next-generation solar devices. Their tunable bandgaps, low-temperature solution-based fabrication, and potential for flexibility and transparency further distinguish them from conventional photovoltaic technologies and make them attractive for a wide range of future energy applications.

This review has shown that the rapid development of PSCs has been driven by continuous advances in material composition, device architecture, and fabrication strategies. Innovations in

electron transport layers, hole transport layers, interface engineering, and compositional tuning have all contributed significantly to improvements in efficiency and stability. At the same time, scalable fabrication methods such as doctor-blade coating, inkjet printing, and roll-to-roll processing have demonstrated the potential to move PSC technology beyond laboratory-scale research toward industrial production.

Despite these achievements, several major challenges continue to hinder the practical and commercial deployment of PSCs. The widespread use of lead-based materials raises important environmental and health concerns, while long-term operational instability under moisture, ultraviolet irradiation, heat, and mechanical stress remains a critical limitation. In addition, a significant gap still exists between the high efficiencies reported under controlled laboratory conditions and the requirements for reliable, large-scale manufacturing. Many fabrication techniques that dominate academic research, particularly spin coating, are not readily suitable for industrial-scale implementation, and comparative studies under realistic operating conditions remain limited.

Furthermore, the review indicates that future progress should not focus solely on the perovskite absorber layer, but also on the synergistic optimization of charge transport materials, interfacial passivation, encapsulation strategies, and overall device engineering. The development of lead-free perovskite systems, tandem cell integration, and more robust 2D/3D hybrid structures represents an important direction for achieving higher efficiency, improved durability, and safer commercialization.

In conclusion, PSCs remain a transformative technology in the global renewable energy landscape. However, achieving industrial viability will require not only continued progress in materials science, but also stronger emphasis on manufacturing scalability, standardized testing protocols, long-term reliability assessment, electrical modeling, and intelligent monitoring systems. A holistic and interdisciplinary approach is therefore essential to translate PSCs from high-performing laboratory devices into commercially viable, stable, and scalable solar energy technologies.

#### **Disclosure statement**

No potential conflict of interest was reported by the author(s).

#### **ACKNOWLEDGEMENT**

This research was not funded by any grant

#### **REFERENCES**

- [1] X. Zhao and N. G. Park, "Stability issues on perovskite solar cells," *Photonics*, vol. 2, no. 4, pp. 1139–1151, 2015, doi: 10.3390/photonics2041139.
- [2] A. H. Ali, R. A. El-Kammar, H. F. Ali Hamed, A. A. Elbaset, and A. Hossam, "Smart monitoring technique for solar cell systems using internet of things based on NodeMCU ESP8266 microcontroller," *Int. J. Electr. Comput. Eng.*, vol. 14, no. 2, pp. 2322–2329, 2024, doi: 10.11591/ijece.v14i2.pp2322-2329.
- [3] P. Roy, N. Kumar Sinha, S. Tiwari, and A. Khare, "A review on perovskite solar cells: Evolution of architecture, fabrication techniques, commercialization issues and status," *Sol. Energy*, vol. 198, no. December 2019, pp. 665–688, 2020, doi: 10.1016/j.solener.2020.01.080.
- [4] S. Kamalakkannan and D. Kirubakaran, "Solar energy based impedance-source inverter for grid system," *Int. J. Electr. Comput. Eng.*, vol. 9, no. 1, pp. 102–108, 2019, doi: 10.11591/ijece.v9i1.pp102-108.
- [5] D. Zhou, T. Zhou, Y. Tian, X. Zhu, and Y. Tu, "Perovskite-Based Solar Cells: Materials, Methods, and Future Perspectives," *J. Nanomater.*, vol. 2018, 2018, doi: 10.1155/2018/8148072.

- [6] M. A. El-Dabah, R. A. El-Sehiemy, M. A. Ebrahim, Z. Alaas, and M. M. Ramadan, "Identification study of solar cell/module using recent optimization techniques," *Int. J. Electr. Comput. Eng.*, vol. 12, no. 2, pp. 1189–1198, 2022, doi: 10.11591/ijece.v12i2.pp1189-1198.
- [7] P. T. Nguyen, L. D. Ho, and D. C. Huynh, "Improved YOLOv10 model for detecting surface defects on solar photovoltaic panels," *Int. J. Electr. Comput. Eng.*, vol. 15, no. 3, p. 3319, 2025, doi: 10.11591/ijece.v15i3.pp3319-3331.
- [8] K. A. T. K, S. Y, and M. T, "Organometal halide perovskites as visible-light sensitizers for photovoltaic cells," *J. Am. Chem. Soc.*, vol. 131, no. 17, pp. 6050–6051, 2009.
- [9] K. Kommuri and V. R. Kolluru, "Implementation of modular MPPT algorithm for energy harvesting embedded and IoT applications," *Int. J. Electr. Comput. Eng.*, vol. 11, no. 5, pp. 3660–3670, 2021, doi: 10.11591/ijece.v11i5.pp3660-3670.
- [10] Y. Rong et al., "Challenges for commercializing perovskite solar cells," *Science (80-. )*, vol. 361, no. 6408, 2018, doi: 10.1126/science.aat8235.
- [11] M. A. Green, A. Ho-Baillie, and H. J. Snaith, "The emergence of perovskite solar cells," *Nat. Photonics*, vol. 8, no. 7, pp. 506–514, 2014, doi: 10.1038/nphoton.2014.134.
- [12] J. P. Correa-Baena et al., "Promises and challenges of perovskite solar cells," *Science (80-. )*, vol. 358, no. 6364, pp. 739–744, 2017, doi: 10.1126/science.aam6323.
- [13] A. S. R. Bati, Y. L. Zhong, P. L. Burn, M. K. Nazeeruddin, P. E. Shaw, and M. Batmunkh, "Next-generation applications for integrated perovskite solar cells," *Commun. Mater.*, vol. 4, no. 1, pp. 1–24, 2023, doi: 10.1038/s43246-022-00325-4.
- [14] J. Y. Kim, J. W. Lee, H. S. Jung, H. Shin, and N. G. Park, "High-Efficiency Perovskite Solar Cells," *Chem. Rev.*, vol. 120, no. 15, pp. 7867–7918, 2020, doi: 10.1021/acs.chemrev.0c00107.
- [15] N. K. Elumalai, M. A. Mahmud, D. Wang, and A. Uddin, "Perovskite solar cells: Progress and advancements," *Energies*, vol. 9, no. 11, 2016, doi: 10.3390/en9110861.
- [16] A. K. Jena, A. Kulkarni, and T. Miyasaka, "Halide Perovskite Photovoltaics: Background, Status, and Future Prospects," *Chem. Rev.*, vol. 119, no. 5, pp. 3036–3103, 2019, doi: 10.1021/acs.chemrev.8b00539.
- [17] S. Information, "General Working Principles of CH<sub>3</sub>NH<sub>3</sub>PbX<sub>3</sub> Perovskite Solar Cells," pp. 2–5, 2013.
- [18] M. H. N. Thi, N. Le Thai, T. M. Bui, and T. N. Kieu, "BaAl<sub>1.4</sub>Si<sub>0.6</sub>O<sub>3.4</sub>N<sub>0.6</sub>:Eu<sup>2+</sup> green phosphors' application for improving luminous performance," *Int. J. Electr. Comput. Eng.*, vol. 13, no. 5, pp. 4958–4965, 2023, doi: 10.11591/ijece.v13i5.pp4958-4965.
- [19] M. Hasan, W. H. Alhazmi, W. Zakri, and A. U. Khan, "Parameter estimation and control design of solar maximum power point tracking," *Int. J. Electr. Comput. Eng.*, vol. 12, no. 5, pp. 4586–4598, 2022, doi: 10.11591/ijece.v12i5.pp4586-4598.
- [20] P. Kajal, K. Ghosh, and S. Powar, "Manufacturing Techniques of Perovskite Solar Cells," *Energy, Environ. Sustain.*, pp. 341–364, 2018, doi: 10.1007/978-981-10-7206-2\_16.
- [21] B. J. Huang, C. K. Guan, S. H. Huang, and W. F. Su, "Development of once-through manufacturing machine for large-area Perovskite solar cell production," *Sol. Energy*, vol. 205, no. February, pp. 192–201, 2020, doi: 10.1016/j.solener.2020.05.005.
- [22] N. L. Chang, A. W. Y. Ho-Baillie, D. Vak, M. Gao, M. A. Green, and R. J. Egan, "Manufacturing cost and market potential analysis of demonstrated roll-to-roll perovskite photovoltaic cell processes," *Sol. Energy Mater. Sol. Cells*, vol. 174, no. August 2017, pp. 314–324, 2018, doi: 10.1016/j.solmat.2017.08.038.
- [23] Y. Ogomi et al., "CH<sub>3</sub>NH<sub>3</sub>SnxPb(1-x)I<sub>3</sub> perovskite solar cells covering up to 1060 nm," *J. Phys. Chem. Lett.*, vol. 5, no. 6, pp. 1004–1011, 2014, doi: 10.1021/jz5002117.

- [24] H. S. Kim et al., "Lead iodide perovskite sensitized all-solid-state submicron thin film mesoscopic solar cell with efficiency exceeding 9%," *Sci. Rep.*, vol. 2, pp. 1–7, 2012, doi: 10.1038/srep00591.
- [25] K. Mahmood, B. S. Swain, and H. S. Jung, "Controlling the surface nanostructure of ZnO and Al-doped ZnO thin films using electrostatic spraying for their application in 12% efficient perovskite solar cells," *Nanoscale*, vol. 6, no. 15, pp. 9127–9138, 2014, doi: 10.1039/c4nr02065k.
- [26] J. M. Ball, M. M. Lee, A. Hey, and H. J. Snaith, "Low-temperature processed meso-structured thin-film perovskite solar cells," *Energy Environ. Sci.*, vol. 6, no. 6, pp. 1739–1743, 2013, doi: 10.1039/c3ee40810h.
- [27] J. H. Heo et al., "Efficient inorganic-organic hybrid heterojunction solar cells containing perovskite compound and polymeric hole conductors," *Nat. Photonics*, vol. 7, no. 6, pp. 486–491, 2013, doi: 10.1038/nphoton.2013.80.
- [28] C. C. Zhang et al., "Electric-field assisted perovskite crystallization for high-performance solar cells," *J. Mater. Chem. A*, vol. 6, no. 3, pp. 1161–1170, 2018, doi: 10.1039/c7ta08204e.
- [29] Y. Yang et al., "Bi-functional additive engineering for high-performance perovskite solar cells with reduced trap density," *J. Mater. Chem. A*, vol. 7, no. 11, pp. 6450–6458, 2019, doi: 10.1039/c8ta11925b.
- [30] M. Haider, C. Zhen, T. Wu, G. Liu, and H. M. Cheng, "Boosting efficiency and stability of perovskite solar cells with nickel phthalocyanine as a low-cost hole transporting layer material," *J. Mater. Sci. Technol.*, vol. 34, no. 9, pp. 1474–1480, 2018, doi: 10.1016/j.jmst.2018.03.005.
- [31] X. Liu et al., "17.46% efficient and highly stable carbon-based planar perovskite solar cells employing Ni-doped rutile TiO<sub>2</sub> as electron transport layer," *Nano Energy*, vol. 50, pp. 201–211, 2018, doi: 10.1016/j.nanoen.2018.05.031.
- [32] P. Docampo, J. M. Ball, M. Darwich, G. E. Eperon, and H. J. Snaith, "Efficient organometal trihalide perovskite planar-heterojunction solar cells on flexible polymer substrates," *Nat. Commun.*, vol. 4, pp. 1–6, 2013, doi: 10.1038/ncomms3761.
- [33] J. Tang et al., "High-performance inverted planar perovskite solar cells based on efficient hole-transporting layers from well-crystalline NiO nanocrystals," *Sol. Energy*, vol. 161, no. December 2017, pp. 100–108, 2018, doi: 10.1016/j.solener.2017.12.045.
- [34] I. Mora-Seró, "How Do Perovskite Solar Cells Work?," *Joule*, vol. 2, no. 4, pp. 585–587, 2018, doi: 10.1016/j.joule.2018.03.020.
- [35] N. Marinova, S. Valero, and J. L. Delgado, "Organic and perovskite solar cells: Working principles, materials and interfaces," *J. Colloid Interface Sci.*, vol. 488, pp. 373–389, 2017, doi: 10.1016/j.jcis.2016.11.021.
- [36] G. E. Eperon et al., "Perovskite-perovskite tandem photovoltaics with optimized band gaps," *Science (80-. )*, vol. 354, no. 6314, pp. 861–865, 2016, doi: 10.1126/science.aaf9717.
- [37] D. T. Moore et al., "Crystallization kinetics of organic-inorganic trihalide perovskites and the role of the lead anion in crystal growth," *J. Am. Chem. Soc.*, vol. 137, no. 6, pp. 2350–2358, 2015, doi: 10.1021/ja512117e.
- [38] N. J. Jeon, J. H. Noh, Y. C. Kim, W. S. Yang, S. Ryu, and S. Il Seok, "Solvent engineering for high-performance inorganic-organic hybrid perovskite solar cells," *Nat. Mater.*, vol. 13, no. 9, pp. 897–903, 2014, doi: 10.1038/nmat4014.
- [39] N. J. Jeon et al., "Compositional engineering of perovskite materials for high-performance solar cells," *Nature*, vol. 517, no. 7535, pp. 476–480, 2015, doi: 10.1038/nature14133.
- [40] Y. Wu et al., "Retarding the crystallization of PbI<sub>2</sub> for highly reproducible planar-structured perovskite solar cells via sequential deposition," *Energy Environ. Sci.*, vol. 7, no. 9, pp. 2934–2938, 2014, doi: 10.1039/c4ee01624f.

- [41] A. Mei et al., "A hole-conductor-free, fully printable mesoscopic perovskite solar cell with high stability," *Science* (80-. ), vol. 345, no. 6194, pp. 295–298, 2014, doi: 10.1126/science.1254763.
- [42] Y. Deng, E. Peng, Y. Shao, Z. Xiao, Q. Dong, and J. Huang, "Scalable fabrication of efficient organolead trihalide perovskite solar cells with doctor-bladed active layers," *Energy Environ. Sci.*, vol. 8, no. 5, pp. 1544–1550, 2015, doi: 10.1039/c4ee03907f.
- [43] H. C. Hsieh, J. Yu, S. P. Rwei, K. F. Lin, Y. C. Shih, and L. Wang, "Ultra-compact titanium oxide prepared by ultrasonic spray pyrolysis method for planar heterojunction perovskite hybrid solar cells," *Thin Solid Films*, vol. 659, no. 2017, pp. 41–47, 2018, doi: 10.1016/j.tsf.2018.05.002.
- [44] M. Hirasawa, T. Ishihara, T. Goto, K. Uchida, and N. Miura, "Magnetoabsorption of the lowest exciton in perovskite-type compound (CH<sub>3</sub>NH<sub>3</sub>)PbI<sub>3</sub>," *Phys. B Phys. Condens. Matter*, vol. 201, no. C, pp. 427–430, 1994, doi: 10.1016/0921-4526(94)91130-4.
- [45] T. Minemoto and M. Murata, "Device modeling of perovskite solar cells based on structural similarity with thin film inorganic semiconductor solar cells," *J. Appl. Phys.*, vol. 116, no. 5, 2014, doi: 10.1063/1.4891982.
- [46] D. B. Mitzi, K. Chondroudis, and C. R. Kagan, "Organic-inorganic electronics," *IBM J. Res. Dev.*, vol. 45, no. 1, pp. 29–45, 2001, doi: 10.1147/rd.451.0029.
- [47] D. B. Mitzi, S. Wang, C. A. Feild, C. A. Chess, and A. M. Guloy, "Conducting Layered Organic-inorganic Halides Containing <110> -Oriented Perovskite Sheets," *Science* (80-. ), vol. 267, no. 5203, pp. 1473–1476, 1995, doi: 10.1126/science.267.5203.1473.
- [48] J. H. Im, C. R. Lee, J. W. Lee, S. W. Park, and N. G. Park, "6.5% Efficient Perovskite Quantum-Dot-Sensitized Solar Cell," *Nanoscale*, vol. 3, no. 10, pp. 4088–4093, 2011, doi: 10.1039/c1nr10867k.
- [49] J. Burschka et al., "Sequential deposition as a route to high-performance perovskite-sensitized solar cells," *Nature*, vol. 499, no. 7458, pp. 316–319, 2013, doi: 10.1038/nature12340.
- [50] E. H. Jung et al., "Efficient, stable and scalable perovskite solar cells using poly(3-hexylthiophene)," *Nature*, vol. 567, no. 7749, pp. 511–515, 2019, doi: 10.1038/s41586-019-1036-3.
- [51] "solar-photovoltaic-panels-christian-jardine[6] جدول."
- [52] M. A. Green et al., "Solar cell efficiency tables (Version 61)," *Prog. Photovoltaics Res. Appl.*, vol. 31, no. 1, pp. 3–16, 2023, doi: 10.1002/pip.3646.
- [53] R. M. Programme, "A UK foresight study of materials in decarbonisation technologies : the case of photovoltaic cells".
- [54] P. J. Dale and M. A. Scarpulla, "Efficiency versus effort: A better way to compare best photovoltaic research cell efficiencies?," *Sol. Energy Mater. Sol. Cells*, vol. 251, no. October 2022, p. 112097, 2023, doi: 10.1016/j.solmat.2022.112097.
- [55] International Renewable Energy Agency, *Renewables Readiness Assessment the Kyrgyz Republic*. 2022.
- [56] T. O. Babarinde, O. S. Ohunakin, D. S. Adelekan, S. A. Aasa, and S. O. Oyedepo, "Experimental study of LPG and R134a refrigerants in vapor compression refrigeration," *Int. J. Energy a Clean Environ.*, vol. 16, no. 1–4, pp. 71–80, 2015, doi: 10.1615/InterJEnerCleanEnv.2016015644.
- [57] K. Ferkous, F. Chellali, A. Kouzou, and B. Bekkar, "Wavelet-Gaussian process regression model for forecasting daily solar radiation in the Saharan climate," *Clean Energy*, vol. 5, no. 2, pp. 316–328, 2021, doi: 10.1093/ce/zkab012.